






The Effect of a Phase Change During the Deposition Stage in Fused Filament Fabrication

S. F. Costa¹ , F. M. Duarte² , and J. A. Covas² 

¹ Center for Research and Innovation in Business Sciences and Information Systems (CIICESI), School of Management and Technology, Porto Polytechnic Institute, Felgueiras, Portugal
sfc@estg.ipp.pt

² Department of Polymer Engineering, Institute for Polymers and Composites (IPC), University of Minho, Guimarães, Portugal
{fduarte, jcovas}@dep.uminho.pt

Abstract. Additive Manufacturing Techniques such as Fused Filament Fabrication (FFF) produce 3D parts with complex geometries directly from a computer model without the need of using molding tools. Due to the rapid growth of these techniques, researchers have been increasingly interested in the availability of strategies, models or data that may assist process optimization. In fact, 3D parts often exhibit limited mechanical performance, which is usually the result of poor bonding between adjacent filaments. In turn, the latter is influenced by the temperature field history during deposition. This study aims at evaluating the influence of considering a phase change from the melt to the solid state on the heat transfer during the deposition stage, as undergone by semi-crystalline polymers. The energy equation considering solidification is solved analytically and then inserted in the MatLab® code previously developed by the authors to model cooling in FFF. The predictions of temperature evolution during the deposition of a simple 3D part demonstrate the importance of that thermal condition and highlight the influence of the type of material used for FFF.

Keywords: Fused Filament Fabrication (FFF) · Phase change · Modelling · Heat transfer

1 Introduction

Additive Manufacturing (AM) is a group of technologies that produces three-dimensional physical objects by gradually adding material [1]. Since the 1980s these technologies became adopted for a growing number of medical/engineering applications and have gradually entered our lives with the development of low-cost 3D printers. In Fused Filament Fabrication (FFF), parts are made layer by layer, each layer being obtained by the extrusion through a nozzle and continuous deposition of a molten plastic filament. The nozzle movements are controlled by a computer, in accordance with a previously defined deposition sequence. Thus, FFF can produce a prototype or a finished product from a Computer Aided Design (CAD) model without the use of molds.

A relative limited range of materials is commercially available for FFF. Acrylonitrile Butadiene Styrene (ABS) and Polylactic Acid (PLA) are the most popular. ABS exhibits good impact resistance and toughness, heat stability, chemical resistance and long service life [2, 3]. PLA is biodegradable (compostable) and has low melting temperature [4, 5]. Several authors compared the performance of the two materials in terms of dimensional accuracy, surface roughness [6] and emission of volatile organic compounds (VOC) [7]. For example, Mudassir [8] proposed a methodology to select among the two materials. Nevertheless, 3D printed parts often show insufficient mechanical performance [9]. This is generally due to insufficient bonding between adjacent filaments, which in turn is determined by the temperature history upon cooling [10]. Consequently, knowledge of the temperature evolution during the deposition/cooling stage is valuable for process set-up and optimization. In a previous work, the authors developed a simulation method to predict the temperature history at any location of a 3D part. This entailed the development of an algorithm to define/up-date automatically contacts and thermal/initial conditions as the deposition proceeds, as well as a criterion to compute the adhesion degree between adjacent filaments [11]. Despite the practical usefulness and the general good agreement between theoretical predictions and experimental data [12], the method can only be used for amorphous materials, such as ABS, which do not exhibit a phase transition from the melt to the solid state. In the case of partially crystalline polymers like PLA, the enthalpy of fusion (also known as latent heat of fusion), must be considered.

The objective of this work is to consider a phase change in the calculation of the temperature evolution during deposition and cooling of FFF parts, and to estimate the magnitude of its effect by comparing the temperature evolution for simple ABS and PLA parts. Once this is accomplished, temperature predictions can be made for the increasing range of materials used in FFF, in order to better understand correlations between processing conditions, material characteristics and printed part properties. The paper is organized as follows. Section 2 presents the algorithm for dealing with cooling materials with a phase change and the resulting computer code. Section 3 considers the deposition and cooling of a single filament and of a simple 3D part to illustrate the differences in cooling of amorphous and semi-crystalline polymers.

2 A Code for the Prediction of Temperatures and Adhesion

2.1 Available Code

It has been shown that during the deposition of a filament, the heat transfers by convection with the environment and by conduction with the support/adjacent filaments control its temperature history [13]. The corresponding energy balance can then be translated into a differential energy equation, which is analytically solved yielding a mathematical expression to compute the temperature evolution with the time [14]. In the simulation method developed by the authors, this expression is used by an algorithm developed using the MatLab, which activates/deactivates automatically contacts and thermal conditions depending on the part geometry, deposition sequence and operating conditions. By coupling an adhesion criteria to the temperature profile history

it is also possible to predict the degree of adhesion between adjacent filaments (Fig. 1) [11]. Then, the objective is now to include an algorithm for the phase change, to make possible the study of parts fabricated from partially crystalline polymers.

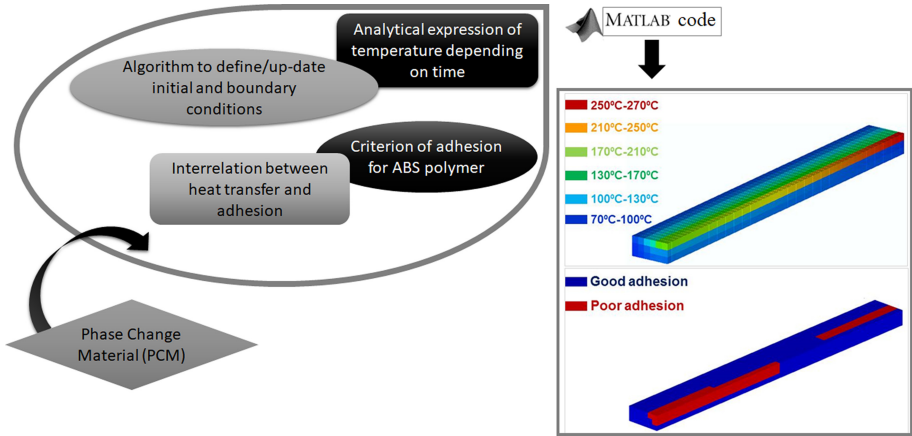


Fig. 1. Diagram of the algorithm to predict temperatures and adhesion of amorphous parts made by FFF.

2.2 Insertion of a Phase Change

When a molten filament made of a partially-crystalline polymer cools down, eventually a phase change from liquid to solid occurs during the time interval $[\tau_l, \tau_s]$, where τ_l is the instant at which the filament reaches the solidification temperature T_{solid} and τ_s is the end of the phase change (Fig. 2).

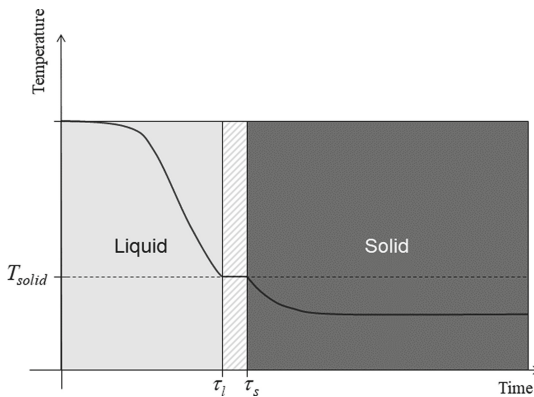


Fig. 2. Typical temperature evolution when a phase change occurs.

If N is the total number of deposited filament segments, the following phase change condition can be defined in the interval $\Delta t = \tau_s - \tau_l$, for each filament:

$$\left(\begin{array}{c} \text{Heat losses} \\ \text{by} \\ \text{convection} \end{array} + \begin{array}{c} \text{Heat transfer} \\ \text{with adjacent filaments} \\ \text{and/or with support} \end{array} \right) = \left(\begin{array}{c} \text{Heat released} \\ \text{during solidification} \end{array} \right) \quad (1)$$

An equation can be written for the r^{th} deposited filament segment ($r \in \{1, \dots, N\}$):

$$\left[h_{conv}(A_r)_{conv}(T_{solid} - T_E) + \sum_{i=1}^n h_i(A_r)_i(T_{solid} - (T_r)_i) \right] \Delta t = m\lambda \quad (2)$$

where h_{conv} is the convective heat transfer coefficient ($W/m^2 \text{ } ^\circ C$), T_E is the environment temperature ($^\circ C$), n is the number of physical contacts of the filament with adjacent filament segments or with the support, h_i is the thermal contact conductance for contact i ($W/m^2 \text{ } ^\circ C$), $(T_r)_i$ is the temperature of the adjacent filament segment or support for contact i ($^\circ C$), m is the mass of the filament segment (kg), λ is the latent heat of fusion (J/kg), $(A_r)_{conv}$ is the area exposed to the environment (m^2) and $(A_r)_i$ is the area of contact i for the r^{th} filament segment (m^2), which are given by:

$$\begin{cases} (A_r)_{conv} = PL(1 - \sum_{i=1}^n (a_r)_i \alpha_i), \forall i \in \{1, \dots, n\} \\ (A_r)_i = PL(a_r)_i \alpha_i \end{cases} \quad (3)$$

P is the cross-section perimeter (m), L is the filament segment length (m), α_i is the fraction of P that is in contact with another segment or with the support and $(a_r)_i$ is defined by, $\forall i \in \{1, \dots, n\}, \forall r \in \{1, \dots, N\}$:

$$(a_r)_i = \begin{cases} 1, & \text{if the } r^{th} \text{ filament segment has the } i^{th} \text{ contact} \\ 0, & \text{otherwise} \end{cases} \quad (4)$$

By using the expressions of $(A_r)_{conv}$ and $(A_r)_i$:

$$\left[h_{conv}PL(1 - \sum_{i=1}^n (a_r)_i \alpha_i)(T_{solid} - T_E) + \sum_{i=1}^n h_i PL(a_r)_i \alpha_i(T_{solid} - (T_r)_i) \right] \Delta t = \rho AL\lambda \quad (5)$$

where ρ is density (kg/m^3) and A is the cross-section area (m^2). Simplifying Eq. 5, an expression for τ_s is obtained:

$$\tau_s = \tau_l + \frac{\rho A \lambda}{h_{conv}P(1 - \sum_{i=1}^n (a_r)_i \alpha_i)(T_{solid} - T_E) + \sum_{i=1}^n h_i P(a_r)_i \alpha_i(T_{solid} - (T_r)_i)} \quad (6)$$

When inserting the phase change in the simulation method, some assumptions must be made:

1. When the computed temperature of the r^{th} filament segment reaches T_{solid} , the thermal conditions used to compute the value of τ_s are the thermal conditions activated at the instant τ_i ;
2. If $((T_r)_i)_0$ is the temperature of the adjacent filament segment for contact i at instant τ_i , the value of $(T_r)_i$ will be assumed as the average between $((T_r)_i)_0$ and T_E ;
3. If during a phase change a filament contacts a new hotter filament, the phase change is interrupted and temperatures are re-computed. When its temperature reaches once more the solidification temperature T_{solid} , τ_s is computed with the new thermal conditions;
4. The crystallization growth does not affect the thermal properties, which are also taken as independent of temperature.

Equation (6) and the assumptions above were inserted in the algorithm. At each time increment, the filaments starting a phase change are identified. The temperature of those filaments suffering a phase change is kept constant unless a new adjacent filament interrupts the process. A simplified flowchart is presented in Fig. 3.

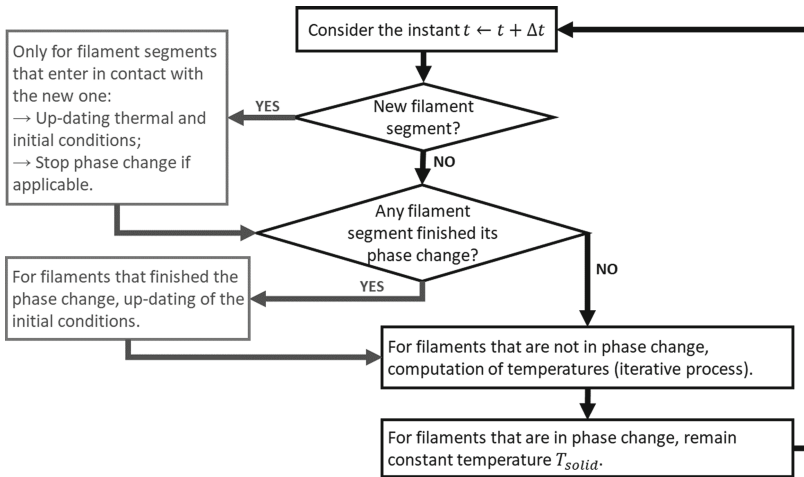


Fig. 3. Simplified flowchart of the section of the code dealing with the phase change.

3 Examples

The first example concerns the deposition of a single filament (Fig. 4.a), while the second deals with the deposition of 10 filaments, where thermal contacts between adjacent filaments develop (Fig. 4.b). Table 1 presents the main properties of the two polymers and Table 2 identifies the process parameters and computational variables.

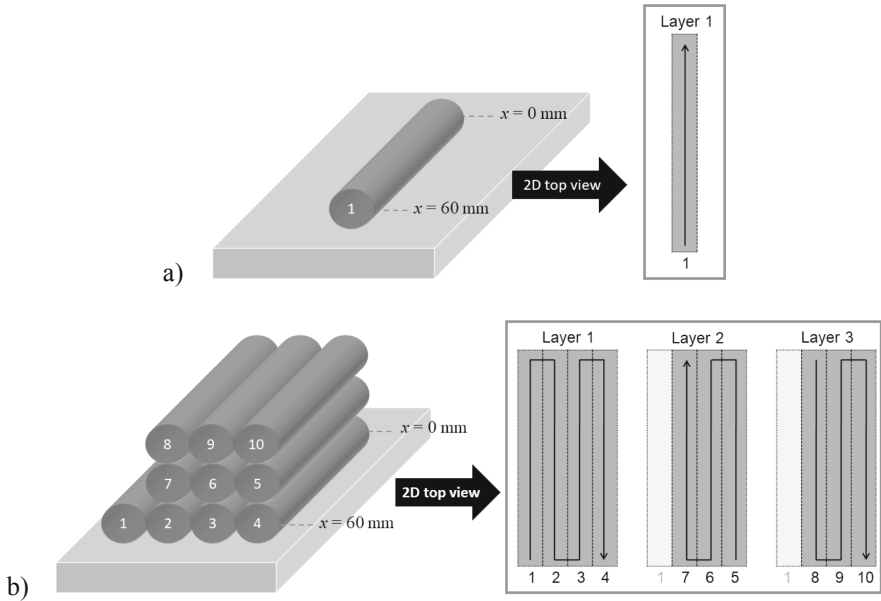


Fig. 4. a) Example 1: deposition of a single filament; b) Example 2: deposition of 10 filaments.

Table 1. Material properties.

Property	ABS	PLA
Density (kg/m^3)	$\rho = 1050$	$\rho = 1300$
Thermal conductivity ($\text{W/m } ^\circ\text{C}$)	$k = 0.2$	$k = 0.1$
Specific heat ($\text{J/kg } ^\circ\text{C}$)	$C = 2020$	$C = 2100$
Latent heat (J/kg)	–	$\lambda = 30\,000$
Solidification temperature ($^\circ\text{C}$)	–	$T_{\text{solid}} = 150$

Figure 5 shows the temperature evolution of a single PLA filament, with and without phase change (at $x = 30$ mm, i.e., at the middle of filament). The phase change starts at $t = 3.25$ s and lasts 0.75 s. During this period the temperature remains constant, whereas it decreases continuously if the phase change is not considered. This results in a temperature difference of 13.9 $^\circ\text{C}$ (at $t = 4$ s) between the two temperatures.

When 10 filaments are deposited, contacts with adjacent filaments and support arise. Figure 6 shows the temperature evolution of filament 2 at $x = 30$ mm, with and without phase change, by considering the PLA material. The phase change occurs at $t = 3.68$ s and lasts 0.4 s, due to the thermal contacts with filaments 1 and 3. The peak initiated at $t = 10$ s is created by the new thermal contact with filament 7. The maximum temperature difference of 18.9 $^\circ\text{C}$ between the two curves is observed at approximately $t = 8$ s. This difference is higher than in the previous example due to the contacts between filaments. As the temperature remains constant during the phase

Table 2. Process and computational parameters.

Property	Value
<i>Process parameters</i>	
Extrusion temperature (°C)	$T_L = 230$
Environment temperature (°C)	$T_E = 25$
Deposition velocity (mm/s)	30
Convective heat transfer coefficient ($W/m^2 \text{ } ^\circ C$) – Natural convection	$h_{conv} = 30$
Thermal contact conductance between adjacent filaments ($W/m^2 \text{ } ^\circ C$)	$h_i = 200$
Thermal contact conductance between filaments and support ($W/m^2 \text{ } ^\circ C$)	$h_i = 10$
Fraction of contact length	$\alpha_i = 0.2$
Filament length (mm)	60
Filament cross-section geometry	<i>circle</i>
Filament cross-section diameter (mm)	0.25
Deposition sequence	Unidirectional and aligned
<i>Computational parameters</i>	
Time increment (s)	0.01
Temperature convergence error (°C)	0.001

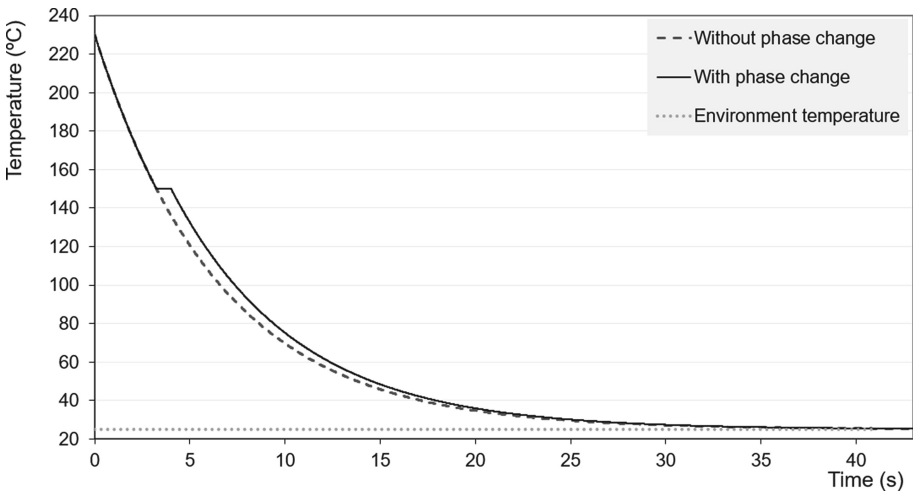


Fig. 5. Evolution of temperature with time for a single PLA filament with and without phase change (at $x = 30$ mm from the edge).

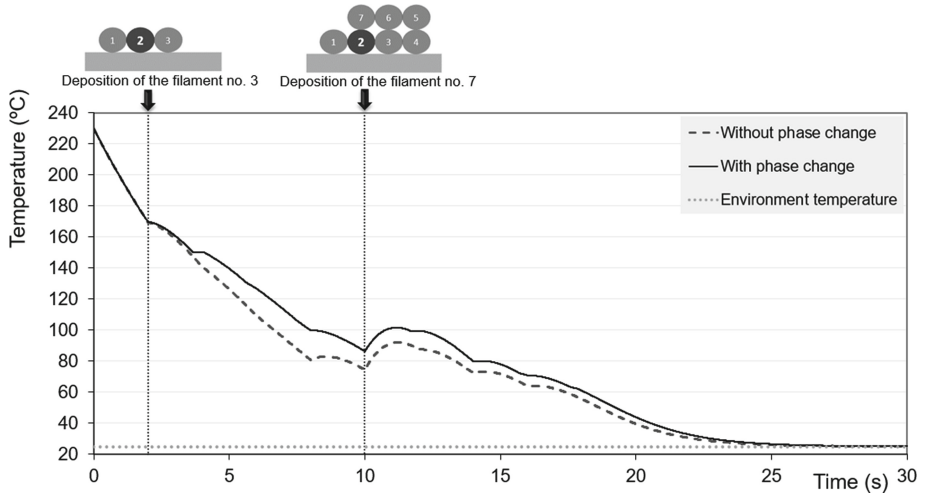


Fig. 6. Evolution of temperature with time for filament no. 2 with and without phase change (at $x = 30$ mm from the edge).

change, those filaments that are in contact with filaments that are under changing phase cool slower, i.e., the temperature of each filament is influenced by its own phase change and by the phase change of the other filaments.

Figure 7 shows the temperature evolution of filament 2, at $x = 30$ mm, for the ABS and PLA materials, with the properties presented in Table 1. The ABS filament cools faster, with a maximum temperature difference of $39.1\text{ }^{\circ}\text{C}$ at approximately $t = 6$ s. This means that this PLA is a better option for FFF, as slower cooling favors adhesion between filaments.

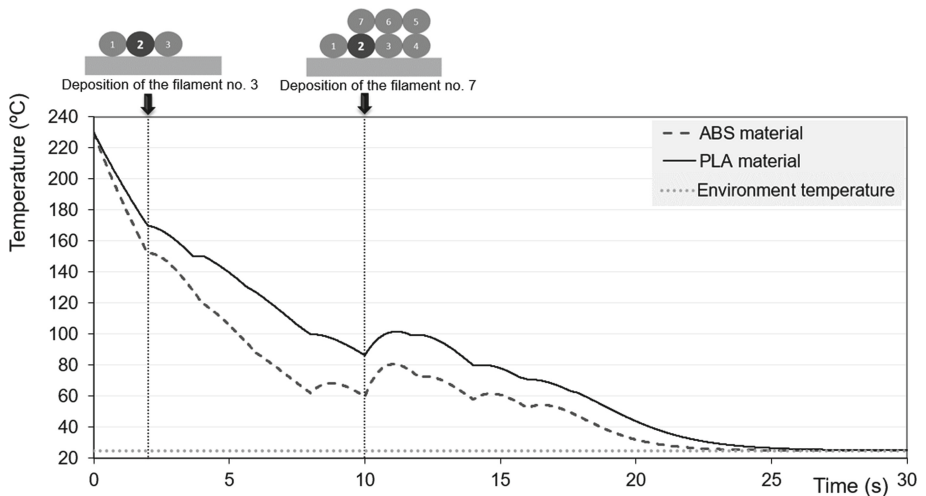


Fig. 7. Evolution of temperature with time for filament no. 2 for ABS and PLA (at $x = 30$ mm from the edge).

4 Conclusions

A simulation method to predict the temperature evolution of filaments during deposition and cooling in FFF, capable of dealing with both amorphous and semi-crystalline polymers, was implemented. The differences between the two types of materials were highlighted with two examples, by using ABS and PLA polymers. The evolution of temperature with time can become significantly different, especially when several filaments become in contact with each other.

The work presented is a first step towards predicting the properties of parts produced by FFF. Knowing the evolution of temperature with time as the deposition stage proceeds, it is possible to predict bonding between contiguous filaments by means of an healing criterion, as well as part shrinkage and warpage arising due to local temperature gradients. As a further step, the mechanical properties of 3D parts could be estimated, for example, with the use of sintering models.

Acknowledgments. This work has been supported by national funds through FCT – Fundação para a Ciência e Tecnologia through project UIDB/04728/2020.

References

1. Gebhardt, A.: Understanding Additive Manufacturing: Rapid Prototyping - Rapid Tooling - Rapid Manufacturing, 1st edn. Edition Hanser, Munich (2012)
2. Izdebska, J.: Printing on Polymers: Theory and Practice. In: Izdebska, J., Thomas, S. (eds.) *Printing on Polymers: Fundamentals and Applications*, pp. 1–20. William Andrew, Waltham (2016)
3. Rodríguez-Panes, A., Claver, J., Camacho, A.M.: The influence of manufacturing parameters on the mechanical behaviour of PLA and ABS pieces manufactured by FDM: a comparative analysis. *Materials* **11**(8), 1–21 (2018)
4. Milde, J., Hrusecky, R., Zaujec, R., Morovic, L., Gorog, A.: Research of ABS and PLA materials in the process of fused deposition modeling method. In: Katalinic, B. (eds.) *Proceedings of the 28th DAAAM International Symposium*, Vienna, Austria, pp. 812–820. DAAM International (2017)
5. Kuznetsov, V.E., Solonin, A.N., Urzhumtsev, O.D., Schilling, R., Tavitov, A.G.: Strength of PLA components fabricated with fused deposition technology using a desktop 3D printer as a function of geometrical parameters of the process. *Polymers* **10**(3), 313–323 (2018)
6. Hafsa, M., Ibrahim, M., Wahab, M., Zahid, M.: Evaluation of FDM pattern with ABS and PLA material. *Appl. Mech. Mater.* **465–466**, 55–59 (2013)
7. Wojtyła, S., Klama, P., Baran, T.: Is 3D printing safe? Analysis of the thermal treatment of thermoplastics: ABS, PLA, PET, and nylon. *J. Occup. Environ. Hyg.* **14**(6), 80–85 (2017)
8. Mudassir, A.: *Measuring accuracy of two 3D Printing Materials*, Department of Engineering Technologies, Bowling Green State University, Bowling Green (2016)
9. Sood, A.K., Ohdar, R.K., Mahapatra, S.S.: Parametric appraisal of mechanical property of fused deposition modelling processed parts. *Mater. Des.* **31**, 287–295 (2010)
10. Sun, Q., Rizvi, G.M., Bellehumeur, C.T., Gu, P.: Effect of processing conditions on the bonding quality of FDM polymer filaments. *Rapid Prototyping J.* **14**, 72–80 (2008)
11. Yang, F., Pitchumani, R.: Healing of thermoplastic polymers at an interface under nonisothermal conditions. *Macromolecules* **35**, 3213–3224 (2002)

12. Costa, S.F., Duarte, F.M., Covas, J.A.: Estimation of filament temperature and adhesion development in fused deposition techniques. *J. Mater. Process. Technol.* **245**, 167–179 (2017)
13. Costa, S.F., Duarte, F.M., Covas, J.A.: Thermal conditions affecting heat transfer in FDM/FFE: a contribution towards the numerical modelling of the process. *Virtual Phys. Prototyping* **10**, 1–12 (2014)
14. Costa, S.F., Duarte, F.M., Covas, J.A.: An analytical solution for heat transfer during deposition in extrusion-based 3D printing techniques. In: *Proceedings of the 15th International Conference Computational and Mathematical Methods in Science and Engineering*, pp. 1161–1172 (2015)